ACID PRODUCTION FROM MIXED SULFIDE MINERALS: THE MIXTURE PYRITE/PYRRHOTITE

C.M.V.B. Almeida and B. F. Giannetti

LaFTA - Laboratório de Físico-Química Teórica e Aplicada
Instituto de Ciências Exatas e Tecnologia da Universidade Paulista
R. Dr. Bacelar 1212, Cep 04026-002, São Paulo, Brazil.
e-mail: biafgian@unip-objetivo.br

ABSTRACT

To assess the response of common sulfide minerals to oxidizing conditions, an electrochemical approach was employed, to define the influence of the pyrrhotite content in pyrite/pyrrhotite mixtures. The influence of the galvanic interactions and local pH on the oxidation reaction of pyrite was also investigated. With this purpose, artificial two-mineral electrodes were constructed ranging in concentration from 20-80% pyrrhotite. The resulting cyclic voltammograms were analyzed and relative quantities of oxidation products were evaluated.

INTRODUCTION

Pyrite and pyrrhotite are minerals common in mine environments that cause acid generation. A major cause of acid production in these environments is sulfide mineral weathering. The exposure of reduced sulfide minerals to the environment results in release of weathering products containing acid due to the oxidation and hydrolysis reactions in soil and geologic material under earth surface conditions. Characterization of complex mineral accumulation containing S compounds is therefore critically valuable to waste characterization. However, little is known about the acid generation characteristics of common sulfide mixtures.

The objective of this paper is to define the influence of the pyrrhotite content, galvanic interactions and local pH on the oxidation reaction of pyrite. With this purpose, two-mineral electrodes were constructed ranging in concentration from 20-80% pyrrhotite. The goal of this work was to define the limit conditions, in terms of pyrrhotite content in the mixture, that determine the SO_4^{2-}/S ratio obtained and to describe some parameters which influence this ratio.

EXPERIMENTAL

The ore pyrite and pyrrhotite samples investigated are from Morro Velho Mine, in Nova Lima, Minas Gerais, Brazil. The minerals were hand ground in an agate mortar and pestle. This material was then sieved to isolate the fraction containing particles < 210 μm, in size.

Potentiodynamic measurements were carried out in a standard electrochemical cell. The carbon paste electrodes consisted of 1.0 g graphite and 1.2 g paraffin containing 5 mg of ground mineral. The reference electrode was an Ag/AgCl electrode placed in a Luggin-Haber capillary and the counter electrode was a platinized platinum wire of large area. The electrolyte buffer, acetic acid/sodium acetate, pH = 4.5 was prepared from Merck p.a. grade reagent and triply distilled water. Nitrogen was bubbled through the cell to deaerate the solution. Potentials values quoted in this text are given on the standard hydrogen scale. All experiments were carried out at 25 °C and scan rate of 20 $mV\ s^{-1}$.

RESULTS AND DISCUSSION

As carbon paste electrodes containing ground mineral were employed, voltammograms of each mineral were performed in order to compare the data obtained with that found in literature. A brief discussion of the processes occurring at each mineral surface is also presented to give support to the results concerning the mixed-mineral electrodes.

Figure 1 shows the cyclic voltammogram obtained from the pyrite carbon paste electrode with the sweep potential starting from the open circuit potential, E_{oc}. The curve obtained is similar to others reported in literature (Halmilton and Woods, 1981; Giannetti et al, 2000) except for the anodic current peak A_1 and the

open circuit potential, which is more negative and corresponds to the system Fe(II)/Fe(III). The carbon paste electrode containing ground mineral can not be polished thus the surface of the pyrite particles may be partially covered by iron oxides/hydroxides formed in air during grinding.

The other aspects of the voltammogram of pyrite are identical to the voltammograms found in literature (Halmilton and Woods, 1981; Giannetti et al, 2000) (Fig. 1). The oxidation reactions of the mineral are fairly discussed in literature and the overall reaction may be represented as:

$$FeS_2 + 8\,H_2O \rightarrow Fe^{3+} + 2\,SO_4^{2-} + 16\,H^+ + 15\,e^- \quad (1)$$

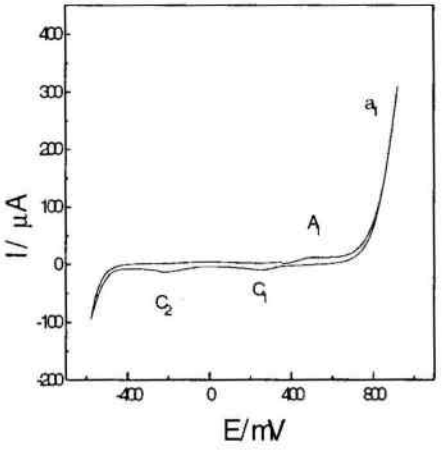

Fig. 1. Voltammogram of pyrite.

In the reverse scan, two current peaks are observed. Peak C_1 was attributed to the reduction of the iron oxides/hydroxides species formed during the oxidation. Peak C_2 was associated to the reduction of sulfur species (Hamilton and Woods, 1981; Yin et al, 1999) in accordance with the following reaction:

$$S + 2H^+ + 2e^- \rightarrow H_2S \quad (2)$$

Figure 2 shows the cyclic voltammogram obtained from the pyrrhotite carbon paste electrode with the sweep potential starting from the open circuit potential, E_{oc}. The curve obtained is similar to that obtained by Hamilton and Woods, 1981. Three anodic current peaks are observed. The anodic dissolution of pyrrhotite results in the formation of ferrous ions and an iron deficient phase. The anodic peak a1 was attributed to the elemental sulfur formation (Hamilton and Woods, 1981):

$$Fe_{(1-x)}S \rightarrow (1-x)\,Fe^{2+} + S + 2\,e^- \quad (3)$$

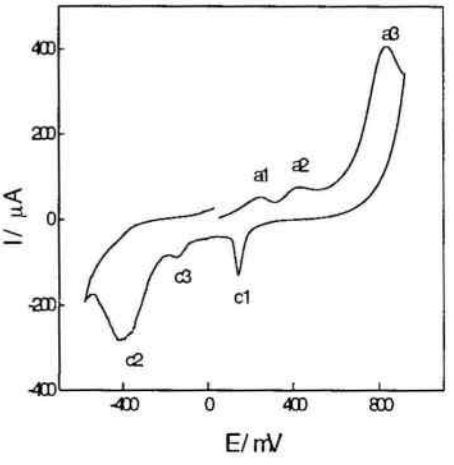

Fig. 2. Voltammogram of pyrrhotite

Increasing the potential, part of the Fe^{2+} is oxidized forming Fe^{3+} (peak a2, at 0.45 V). The anodic current peak a3 may be associated to the oxidation of the intermediates formed (Equation (4)). In the reverse scan (Fig. 2), three cathodic current peaks are observed being c1 related to the reduction of the Fe^{3+}, at 0.2 V.

$$S_2O_3^{2-} + 5\,H_2O \rightarrow 2\,SO_4^{2-} + 10\,H^+ + 8\,e^- \quad (4)$$

Current peaks c2 and c3 had been considered relative to the reduction of the layer rich in sulfur/intermediates at the electrode surface. (Buckley and Woods, 1985).

The two-mineral electrodes were made with pyrite, which has the most known electrochemical behavior and pyrrhotite ranging 20-100% by weight. Fig. 3 shows the effect of the FeS presence on the pyrite voltammogram. Increasing the pyrrhotite content reduces the value of the current a1, i.e., the electrode surface becomes less active. When the pyrrhotite content is greater than 40%, the current peak c3 appears. This peak was previously observed in the voltammogram of pure pyrrhotite and was associated to initial reduction of the layer rich in sulfur. The current peak C_2 (Equation 2) increases significantly indicating that the pyrite/pyrrhotite combination favors the sulfur production.

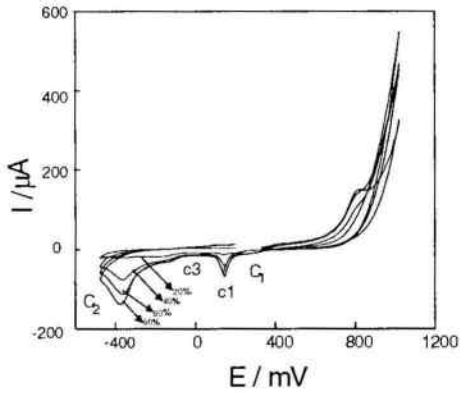

Fig. 3. Cyclic voltammograms of pyrite/pyrrhotite carbon paste electrode.

In order to quantify the oxidation products formed, the charge passed in the anodic and cathodic processes was determined by integration of the area under the voltammograms, on the positive-going and subsequent return scans, at 20 mV s^{-1}. The difference between Q_a and Q_c results from the soluble species formed during oxidation.

The sulfate formed diffuses into solution (Hamilton and Woods, 1981) and its reduction does not occur in the potential range of this study (Flatt and Woods, 1995). Thus, the quantity of SO_4^{2-} formed during oxidation may be evaluated from the difference between the total anodic and cathodic charges. The cathodic charge associated to the reduction of $Fe(OH)_3$ was estimated in the potential range between 0.35 V and 0.05 V (Q_{c1}) and between 0.35 and –0.02 V for pyrrhotite. The charge due to reaction (2) was obtained between -0.06 V and -0.4 V (Q_{c2}) for pyrite and between –0.06 V and –0.5 V for pyrrhotite. As the charge values so obtained include the contribution of both minerals decomposition, the value of the charge transferred during the negative-going scan, beginning at E_{oc} was subtracted over this potential range.

The area of the carbon paste electrodes is unknown. Thus, to evaluate the quantities of SO_4^{2-}, S and $Fe(OH)_3$ produced by the electrodes, relative quantities of soluble compounds, ferric hydroxide, and elemental sulfur were calculated as shown in table 1.

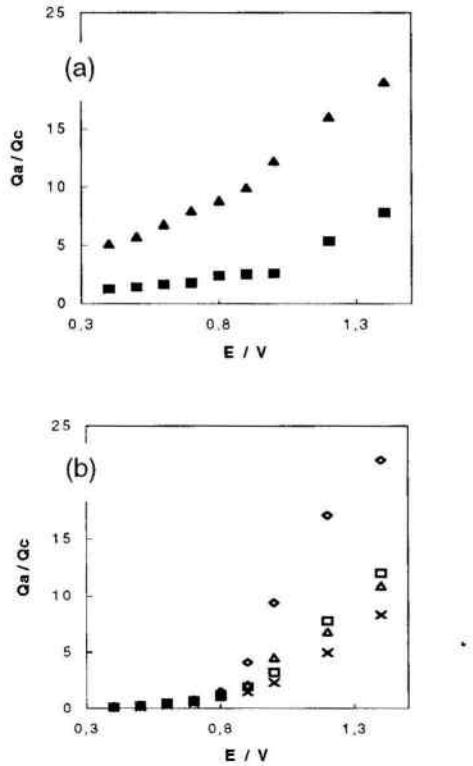

Fig. 4. Dependence of the ratio Q_a/Q_c on the anodic potential limit: (▲) pyrite alone, (■) pyrrhotite alone and pyrite plus: (✧) 20% pyrrhotite, (□) 40% pyrrhotite, (Δ) 60% pyrrhotite and (x) 80% pyrrhotite.

Figure 4 shows the variation of the Q_a/Q_c ratio with the anodic end point potential, $E_{\lambda a}$, for pyrite and pyrrhotite electrodes (a) and for the two-mineral electrodes (b). For potentials more negative than 0.8 V, the two-mineral electrodes are less active than the pure mineral electrodes and, despite of the surface composition, produce similar quantities of soluble products. There is no linear relationship between the activity of the electrodes and the percentage of pyrrhotite.

Tab.1. Evaluation of the relative quantities of oxidation products generated by the two-mineral electrodes.

%			E / V
$Fe(OH)_3$	=	(Q_{c1}/Q_a) 100	$E_{ca} \leq E \leq 1,0$ V
S	=	(Q_{c2}/Q_a) 100	$Eca \leq E \leq 1,0$ V
SO_4^{2-}	=	$[(Q_a - Q_c) / Q_a]$ 100	$E \leq 0,85$ V

The pyrite and pyrrhotite electrodes show a decrease of the $\%Fe(OH)_3$ with increasing the potential (Fig. 5). The production of iron hydroxide from the pyrrhotite electrode is more intense than that from the

cathode with 2 mg simulating a single electrode composed by 60% pyrrhotite and 40% pyrite.

(B) a two-mineral electrode was constructed with the anode (60% pyrrhotite) placed next to the cathode (40% pyrite) without homogenization of the minerals.

(C) a two-mineral electrode with mixed 60% pyrrhotite and 40% pyrite.

The results of experiments A, B and C showed that the electrodes short-circuited externally do not produce sulfur comparable to that obtained when a single electrode containing 60% pyrrhotite and 40% pyrite (Tab. 2). Meanwhile the two-mineral electrode presented the expected results. Thus, the increase in sulfur yield is not due to the electrical contact the pyrite/pyrrhotite. This result certainly evidences that conclusions based on single mineral studies may be quite imprecise.

Tab. 2. Dependence of the ratio Qa/Qc and of the relative quantities of oxidation products on electrode type.

electrode	Qa/Qc	% S	% SO_4^{2-}	% $Fe(OH)_3$
(A)	1,70	52	41	7
(B)	1,29	76	22	7
(C)	1,21	74	17	8

A change in local pH should be another factor, which may interfere on the ratio SO_4^{2-}/S as the lack of protons near the electrode could increase the local pH (Paul et al, 1978) favoring the sulfur oxidation to thiosulfate. Measurements of the pH of solutions containing water/pyrite and water/pyrrhotite were carried out in order to verify if a local change of pH could influence the sulfur yield of the two-mineral electrodes. The results are shown in Table 3.

Tab. 3. pH values of aqueous solutions containing 5 g of mineral(s) in 25 ml water.

mineral	pH
pyrite	4,0
20% pyrrhotite / 80% pyrite	4,0
40% pyrrhotite / 60% pyrite	4,0
60% pyrrhotite / 40% pyrite	4,0
80% pyrrhotite / 20% pyrite	4,5
pyrrhotite	4.5

When the pyrite content is greater than 40% there is no change in the pH value in relation to that measured in a solution containing pyrite alone. The dissolution of pyrite results in the production of H^+ ions which can lower the local pH at the electrode surface. Otherwise, the thiosulfate decomposition depends considerably on pH, being the kinetics of sulfur formation a first order reaction in relation to the H^+ concentration.

Comparing the results obtained from pH measurements with that shown in Fig. 8, it can be inferred that in region (I), where the electrodes contain more than 40% pyrite, the local pH decreases and the decomposition of thiosulfate is favored.

Thus, more sulfur than sulfate is produced. In region (II), the pyrrhotite content is greater than 60%, and there is an increase in the local pH disfavoring the thiosulfate decomposition. In addition, when the pyrite content is less than 40%, the higher pH next the surface may promote the oxidation of the sulfur species and hence more sulfate than sulfur is produced (Mycroft et al, 1990). It is worth noting that an increase in iron hydroxide quantity is also noticed when the pyrrhotite content is greater than 60% (Fig. 8). Hamilton and Woods, 1981, reported that the iron oxides/hydroxides inhibit significantly the pyrrhotite oxidation. The film formed would increase the resistance to the charge-transfer process during the mineral dissolution.

CONCLUSIONS

The influence of pyrrhotite content in a pyrite/pyrrhotite electrode was examined:

(1) At potential next to the open circuit potential, the reactions producing sulfur and Fe(III) predominate

(2) The presence of pyrrhotite inhibits sulfate formation

(3) Galvanic interactions occur, but the increase in sulfur yield, when $E < 0.8$ V and % pyrite < 40%, is not due to the electrical contact between pyrite and pyrrhotite.

(4) The presence of more than 40% pyrite in the mixture enhances the H^+ production, which lowers the local pH and favors thiosulfate decomposition. Thus, in this condition more sulfate is produced.

(5) Remediation strategies for disturbed lands containing reduced S minerals must first consider the quantity and the nature of sulfide minerals present.

ACKNOWLEDGEMENTS

Financial support from Fundação de Amparo à Pesquisa do Estado de São Paulo, FAPESP, is gratefully recognized. The authors also thank the support of Vice-Reitoria de Pesquisa e Pós-Graduação da Universidade Paulista.

REFERENCES

Buckley, A. N., Woods, R., 1985. X-Ray photoelectron spectroscopy of oxidised pyrrhotite surfaces, I. Exposure to air. Applic. of Surf. Sci. 22/23, 280-287 and 20, 472-480.

Flatt, J. R., Woods, R., 1995. A voltammetric investigation of the oxidation of pyrite in nitric acid solutions: relation to treatment of refractory gold ores. J. Appl. Electrochem. 25, 852-856.

Giannetti, B. F., Bonilla, S. H., Zinola, C. F., Rabóczkay, T., 2000. Voltammetric and Photoelectrochemical Response of Natural Pyrite in Acetic Acid-Acetate Buffer Solution. Hydrometallurgy, in press.

Hamilton, I.C.; Woods, R., 1981. An Investigation of surface Oxidation of Pyrite and Pyrrhotite by Linear Potential Sweep Voltammetry. J. Electroanal. Chem., 118, 327-343.

Holmes, P. R., Crundwell, F. K., 1995. Kinetic aspects of galvanic interactions between minerals during dissolution. Hydrometallurgy 39, 353-375.

Mishra, K. K., Osseo-Asare, K., 1988. Aspects of the Interfacial Electrochemistry of Semiconductor Pyrite (FeS_2). J. Electrochem. Soc., 135, 2502-2509.

Mycroft, J.R., Bancroft, G.M., McIntyre, N.S., Lorimer, J.W., Hill, I.R., 1990. Detection of Sulfur and Polysulfides on Electrochemically Oxidized Pyrite Surfaces by X-ray Photoelectron-Spectroscopy and Raman-Spectroscopy. J. Electroanal. Chem., 292(1-2), 139-152.

Paul, R. L., Nicol, M. J., Diggle, J. W., Saunders, A. P., 1978. The electrochemical behaviour of galena (Lead Suphide) – I. Anodic dissolution. Electrochim. Acta 23, 625-633.

Yin, Q., Kelsall, G. H., Vaughan, D. J., Welham, N. J., 1999. Rotating Ring(Pt)-Disk(FeS2) Electrode Behaviou in Hydrocloric Acid. J. Colloid. Interf. Sci., 210, 375-383.